

UCLA

UCLA Previously Published Works

Title

TRIF Differentially Regulates Hepatic Steatosis and Inflammation/Fibrosis in Mice

Permalink

<https://escholarship.org/uc/item/0bd4d81p>

Journal

Cellular and Molecular Gastroenterology and Hepatology, 3(3)

ISSN

2352-345X

Authors

Yang, Ling
Miura, Kouichi
Zhang, Bi
et al.

Publication Date

2017-05-01

DOI

10.1016/j.jcmgh.2016.12.004

Peer reviewed

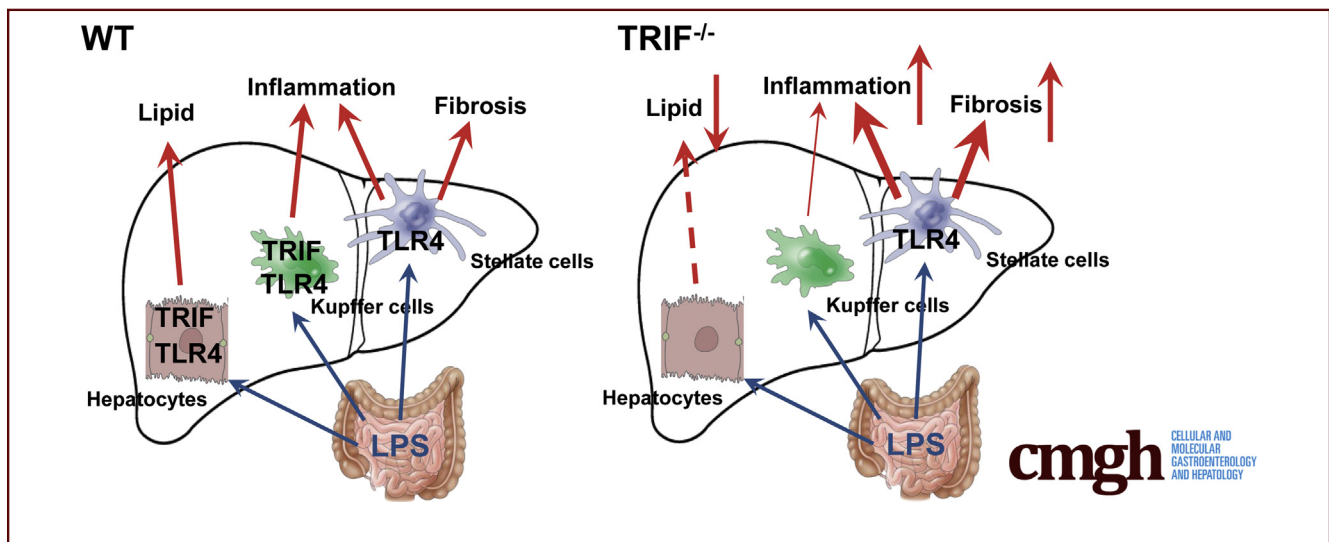
ORIGINAL RESEARCH

TRIF Differentially Regulates Hepatic Steatosis and Inflammation/Fibrosis in Mice



Ling Yang,^{1,2,*} Kouichi Miura,^{1,3,*} Bi Zhang,^{1,*} Hiroshi Matsushita,^{1,4} Yoon Mee Yang,⁴ Shuang Liang,¹ Jingyi Song,¹ Yoon Seok Roh,^{1,4,7} and Ekihiro Seki^{1,4,5,6}

¹Division of Gastroenterology, Department of Medicine, University of California San Diego, School of Medicine, La Jolla, California; ²Division of Gastroenterology, Union Hospital, Tongji Medical College, Huazhong University of Science and Technology, Wuhan, China; ³Department of Gastroenterology, Akita University Graduate School of Medicine, Akita, Japan; ⁴Division of Gastroenterology, Department of Medicine, ⁵Department of Biomedical Sciences, Cedars-Sinai Medical Center, Los Angeles, California; ⁶Department of Medicine, University of California Los Angeles, David Geffen School of Medicine, Los Angeles, California; ⁷Department of Pharmacy, Chungbuk National University College of Pharmacy, Chungbuk, South Korea



SUMMARY

Translocated intestine-derived lipopolysaccharide stimulates Toll-like receptor 4 expressed in different liver cells that have distinct roles in the development of nonalcoholic steatohepatitis. The Toll-like receptor 4-mediated TIR-domain containing adaptor-inducing interferon- β pathway promotes liver steatosis, but inhibits inflammation and fibrosis in nonalcoholic steatohepatitis.

BACKGROUND & AIMS: Toll-like receptor 4 (TLR4) signaling is activated through 2 adaptor proteins: MyD88 and TIR-domain containing adaptor-inducing interferon- β (TRIF). TLR4 and MyD88 are crucial in nonalcoholic steatohepatitis (NASH) and fibrosis. However, the role of TRIF in TLR4-mediated NASH and fibrosis has been elusive. This study investigated the differential roles of TRIF in hepatic steatosis and inflammation/fibrosis.

METHODS: A choline-deficient amino acid defined (CDAA) diet was used for the mouse NASH model. On this diet, the mice develop hepatic steatosis, inflammation, and fibrosis. TLR4 wild-type and TLR4^{-/-} bone marrow chimeric mice and

TRIF^{-/-} mice were fed CDAA or a control diet for 22 weeks. Hepatic steatosis, inflammation, and fibrosis were examined.

RESULTS: In the CDAA diet-induced NASH, the mice with wild-type bone marrow had higher alanine aminotransferase and hepatic tumor necrosis factor levels than the mice with TLR4^{-/-} bone marrow. The nonalcoholic fatty liver disease activity score showed that both wild-type and TLR4^{-/-} bone marrow chimeras had reduced hepatic steatosis, and that both types of chimeras had similar levels of inflammation and hepatocyte ballooning to whole-body wild-type mice. Notably, wild-type recipients showed more liver fibrosis than TLR4^{-/-} recipients. Although TRIF^{-/-} mice showed reduced hepatic steatosis, these mice showed more liver injury, inflammation, and fibrosis than wild-type mice. TRIF^{-/-} stellate cells and hepatocytes produced more C-X-C motif chemokine ligand 1 (CXCL1) and C-C motif chemokine ligand than wild-type cells in response to lipopolysaccharide. Consistently, TRIF^{-/-} mice showed increased CXCL1 and CCL3 expression along with neutrophil and macrophage infiltration, which promotes liver inflammation and injury.

CONCLUSIONS: In TLR4-mediated NASH, different liver cells have distinct roles in hepatic steatosis, inflammation, and fibrosis. TRIF promotes hepatic steatosis but it inhibits injury,

inflammation, and fibrosis. (*Cell Mol Gastroenterol Hepatol* 2017;3:469–483; <http://dx.doi.org/10.1016/j.jcmgh.2016.12.004>)

Keywords: TLR4; Hepatocyte Apoptosis; LPS; Neutrophils.

See editorial on page 299.

Fatty liver disease is the result of excessive fat accumulation in hepatocytes. Nonalcoholic fatty liver disease (NAFLD) is a manifestation of the metabolic syndrome, commonly associated with obesity and insulin resistance. The spectrum of NAFLD ranges from simple steatosis to steatosis accompanied by hepatocyte ballooning, inflammation, and fibrosis, referred to as nonalcoholic steatohepatitis (NASH).^{1–4} NASH can progress to cirrhosis, which significantly increases the risk of hepatocellular carcinoma.^{1–4} To date, there is no effective preventive or therapeutic agent for NASH and its associated fibrosis and hepatocellular carcinoma. Therefore, a better understanding of the underlying molecular mechanism is critical for the development of new and effective therapies.

Consumption of diets containing excessive fat and sugar is a risk factor for metabolic syndrome. These so-called Western-style diets may cause intestinal bacterial overgrowth as well as alter the composition of the intestinal microbiome. The altered intestinal microbiome may participate in endotoxin production, endogenous alcohol production, bile acid metabolism, and choline metabolism. Western-style diets form a gut microbiota that converts dietary choline into methylamines, reducing plasma levels of phosphatidylcholine. Because phosphatidylcholine is required for the secretion of very low density lipoprotein from hepatocytes, reduced choline levels can exacerbate fat accumulation in hepatocytes.⁵

Increased blood lipopolysaccharide (LPS) levels often are observed in patients with NASH.^{5–7} Toll-like receptor 4 (TLR4) is a pattern-recognition receptor for LPS and induces activation of innate immune signaling through adaptor proteins MyD88 and TIR-domain containing adaptor-inducing interferon- β (TRIF).⁸ Previous studies clearly have shown the critical roles of TLR4 and MyD88 in promoting NASH and its related fibrosis.^{9–11} Interestingly, Interferon regulatory factor 3 (IRF3), downstream of the TRIF-dependent pathway, plays paradoxical roles between alcoholic liver disease and high-fat diet (HFD)-induced NAFLD. The TRIF-mediated IRF3 activation promotes alcohol-induced liver injury whereas IRF3 negatively regulates HFD-induced steatosis.^{12,13} However, the precise roles of the TLR4–TRIF pathway in NASH and fibrosis remain elusive.

HFD feeding induces fatty liver, weight gain, and insulin resistance, but liver inflammation is very mild and fibrosis does not occur. In contrast, feeding of a methionine-choline-deficient diet, commonly used for NASH studies in rodents, induces liver injury and inflammation, but body weight is reduced and insulin resistance is not developed. Notably, rodents fed a choline-deficient amino acid defined (CDAA) diet evidently develop fibrosis along with hepatic

steatosis, inflammation, weight gain, and mild insulin resistance.¹⁰ Because we aimed to examine TLR4-mediated NASH fibrosis, this study used CDAA diet feeding to understand the mechanisms of the pathogenesis of NASH fibrosis. The present study investigated to determine the responsible cell types for TLR4-mediated NASH and fibrosis, and the role of TRIF in the development of NASH and its related fibrosis.

Materials and Methods

Mouse Colonies


Wild-type C57BL/6 mice and *Trif*^{flps/flps} mice (hereafter referred to as TRIF^{-/-} mice) were purchased from The Jackson Laboratory (Bar Harbor, MA).¹⁴ TLR4^{-/-} mice and MyD88^{-/-} mice originally were developed in Shizuo Akira's laboratory and were back-crossed to C57BL/6 for more than 10 generations.¹⁵ Male mice were divided into 2 groups at 8 weeks old: choline-supplemented L-amino acid–defined diet (catalog no. 518754; Dyets, Inc, Bethlehem, PA) and CDAA (catalog no. 518753; Dyets, Inc).¹⁰ These diets were continued for 22 weeks. The mice received humane care based on the National Institutes of Health recommendations outlined in the Guide for the Care and Use of Laboratory Animals. All animal experiments were approved by the University of California San Diego and Cedars-Sinai Medical Center Institutional Animal Care and Use Committee.

Bone Marrow Transplantation

We performed bone marrow transplantation (BMT) experiments as previously described.¹⁴ Briefly, bone marrow (BM) cells (1×10^7 cells) obtained from wild-type and TLR4^{-/-} mice were transplanted through tail veins after the recipient mice were lethally irradiated (10 Gy). After 2 weeks of lethal irradiation followed by BMT, liposomal clodronate (200 μ L intravenously) was injected to deplete liver resident macrophages, Kupffer cells, which accelerate hepatic macrophage turnover with BM cells. The mice were fed with CDAA and choline-supplemented amino acid–defined diet after 10 weeks of BMT. These diets were continued for 22 weeks. Some mice were transplanted with BM from β -actin promoter–driven green fluorescent protein (GFP) transgenic mice for assessing the efficiency of the engraftment of transplanted BM cells.

*Authors share co-first authorship.

Abbreviations used in this paper: ALT, alanine aminotransferase; BM, bone marrow; BMT, bone marrow transplantation; CDAA, choline-deficient amino acid defined; DGAT2, diacylglycerol acyltransferase 2; HFD, high-fat diet; HSC, hepatic stellate cell; IL, interleukin; LDH, lactate dehydrogenase; LPS, lipopolysaccharide; NAFLD, nonalcoholic fatty liver disease; NASH, nonalcoholic steatohepatitis; PCR, polymerase chain reaction; α -SMA, α -smooth muscle actin; TLR4, Toll-like receptor 4; TNF, tumor necrosis factor.

 Most current article

© 2017 The Authors. Published by Elsevier Inc. on behalf of the AGA Institute. This is an open access article under the CC BY-NC-ND license (<http://creativecommons.org/licenses/by-nc-nd/4.0/>).

2352-345X

<http://dx.doi.org/10.1016/j.jcmgh.2016.12.004>

Mouse Tissue Processing

Mouse tissues were either snap-frozen in liquid nitrogen for RNA, or fixed in 10% or 4% neutral buffered formalin phosphate (Fisher Scientific, Pittsburgh, PA) to be embedded in paraffin or OCT compound, then cut into 5- μ m sections for H&E, Oil-red O, and Sirius red staining. The Sirius red-positive area was measured on 10 low-power (40 \times) fields/slide and quantified with the use of National Institutes of Health imaging software. NAFLD activity score was determined as described.¹⁰ Immunostaining for α -smooth muscle actin (α -SMA), Ly6G, and F4/80 was performed.¹⁰

Quantitative Real-Time Polymerase Chain Reaction

Extracted RNA from livers and cells was subjected to reverse-transcription and subsequent quantitative real-time polymerase chain reaction (PCR) with the use of the CFX96 real-time PCR system (Bio-Rad, Hercules, CA). PCR primer sequences are listed in Table 1. Genes were normalized to 18S RNA as an internal control.

Cell Isolation and Treatment

Hepatocytes, hepatic stellate cells (HSCs), and Kupffer cells were isolated from the mice as previously described.¹⁴ HSCs were isolated in a 2-step process: collagenase-pronase perfusion of mouse livers followed by 8.2% Nycodenz (Accurate Chemical and Scientific Corporation) 2-layer discontinuous density gradient centrifugation. To ensure the highest possible purity, we depleted contaminated liver macrophages from HSC fractions by magnetic antibody cell sorting (Miltenyi Biotec, San Diego, CA) using an antibody to F4/80 antigen (eBioscience, San Diego, CA) and CD11b-conjugated microbeads (Miltenyi Biotec, San Diego, CA). Kupffer cells were isolated using magnetic antibody cell sorting with antibody to F4/80 antigen (eBioscience, San Diego, CA) and CD11b-conjugated microbeads. After cell attachment, hepatocytes were serum-starved for 16 hours. The culture media for Kupffer cells and HSCs were changed to 1% serum for 16 hours followed by treatment with 200

μ mol/L palmitate, and/or 100 ng/mL LPS. Albumin-conjugated palmitate was prepared as previously described.¹⁶ Apoptosis was examined using terminal deoxynucleotidyl transferase-mediated deoxyuridine triphosphate nick-end labeling staining. Lipid accumulation was assessed by Oil red O staining. The lactate dehydrogenase (LDH) release method was used for cell death quantification. LDH activity was measured in cell culture supernatants and compared with LDH activity of cells lysed in 2% Triton X-100, as suggested by the manufacturer (Roche Molecular Diagnostics, Pleasanton, CA).

Lipid Isolation and Measurement

Liver extracts were prepared by homogenization in 0.25% sucrose with 1 mmol/L EDTA and extracted as previously described.¹⁰ Triglyceride was measured with the use of Triglyceride Reagent Set (Pointe Scientific, Canton, MI). Hepatocyte triglyceride accumulation was quantified by extraction of hepatocyte lipids from cell homogenates using chloroform/methanol (2:1).

Glucose and Insulin Tolerance Tests

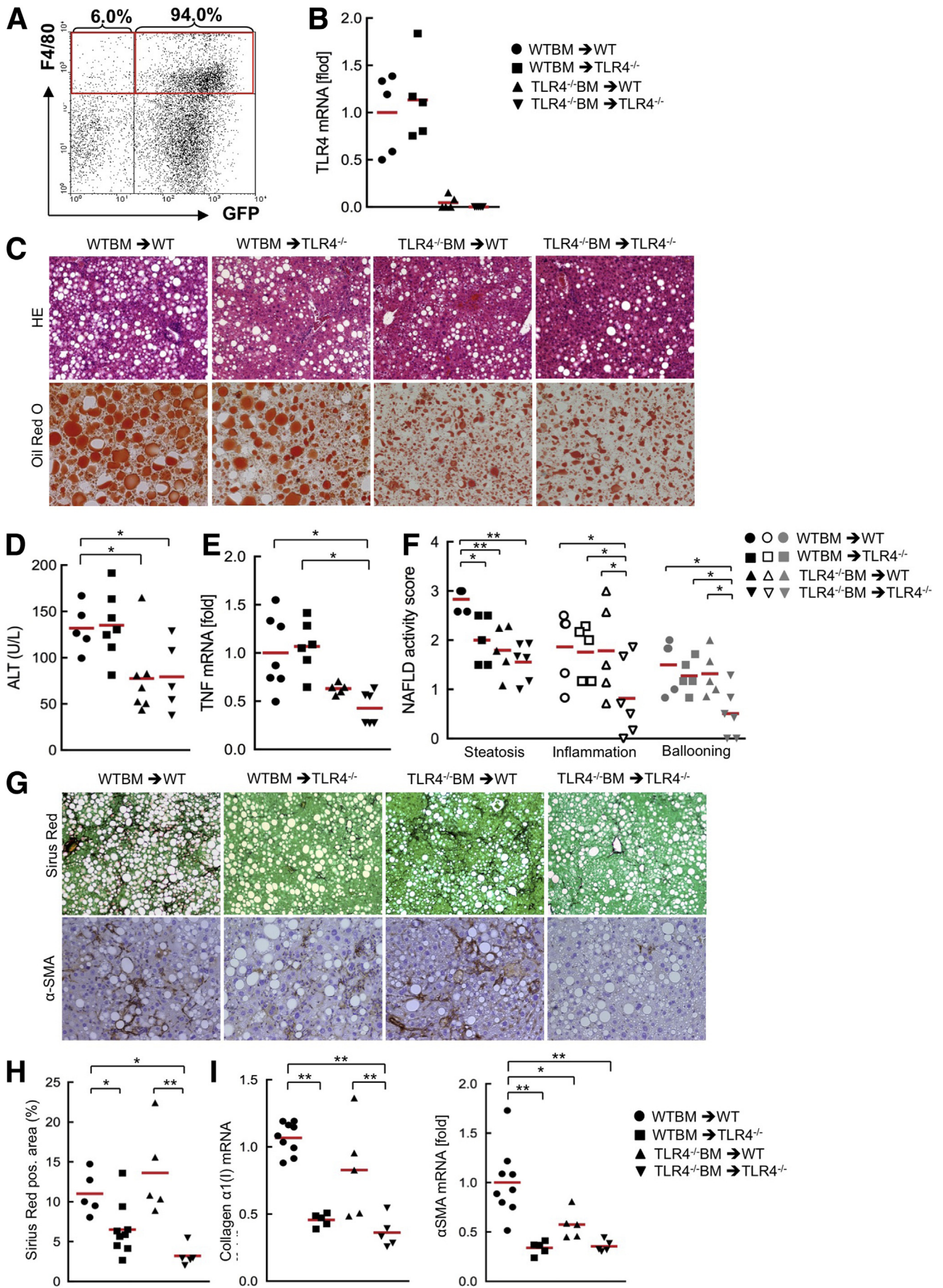
For glucose tolerance test, the baseline glucose levels were measured using mice that had fasted for 16 hours (0 min). Then, 2 g/kg glucose was administered to the mice via intraperitoneal injection, and glucose levels were measured at 15-minute intervals over a span of 2 hours after the glucose load. For the insulin tolerance test, the baseline glucose levels were measured after 4 hours of fasting. The blood glucose concentration was monitored every 15–30 minutes for 90 minutes after 0.5 U/kg of insulin was administered via intraperitoneal injection.

Statistical Analysis

Differences between the 2 groups were compared using the Mann-Whitney *U* test or a 2-tailed unpaired Student *t* test. Differences between multiple groups were compared by 1-way analysis of variance using GraphPad Prism 7

Table 1. Sequence of Primers Used for Real-Time Quantitative PCR

Gene	Forward	Reverse
18s	AGTCCCTGCCCTTTGTACACA	CGATCCGAGGGCCTCACTA
TNF	AGGGTCTGGGCCATAGAACT	CCACCACGCTCTTCTGTCTAC
IL1 β	GGTCAAAGGTTTGAAGCAG	TGTGAAATGCCACCTTTTGA
Collagen α 1(I)	TAGGCCATTGTGTATGCAGC	ACATGTTTCAGCTTTGTGGACC
α -SMA	GTTCAGTGGTGCCTCTGTCA	ACTGGGACGACATGGAAAAG
Timp1	AGGTGGTCTCGTTGATTCT	GTAAGGCCGTAGCTGTGCC
CXCL1	TGCACCCAAACCGAAGTC	GTCAGAAGCCAGCGTTCACC
CCL3	GTGGAATCTTCCGGCTGTAG	ACCATGACACTCTGCAACCA
CCL5	CCACTTCTTCTCTGGGTTGG	GTGCCCACGTCAAGGAGTAT
Bambi	TGAGCAGCATCACAGTAGCA	CGCCACTCCAGCTACTTCTT
IL10	TGTCAAATTCATTCATGGCCT	ATCGATTTCTCCCTGTGAA
DGAT2	GAAGATGTCTTGAGGGGCTG	CGCAGCGAAAACAAGAATAA



software (GraphPad Software, Inc, La Jolla, CA). *P* values less than .05 were considered significant.

Results

Distinct Roles of BM-Derived and Resident Liver Cells in TLR4-Mediated Hepatic Steatosis, Injury, Inflammation, and Fibrosis in CDA Diet-Fed Mice

Kupffer cells, resident liver macrophages, have been suggested to be major players for TLR4-mediated hepatic steatosis and inflammation.¹¹ We previously reported that TLR4 expressed in HSCs plays a crucial role in HSC activation and fibrosis.¹⁴ However, the responsible liver cells and the function of TLR4 in NASH-related fibrosis have not been well documented. To explore the responsible cell types for TLR4-mediated NASH and fibrosis, BM cells from wild-type or TLR4^{-/-} mice were transplanted into wild-type or TLR4^{-/-} recipient mice followed by feeding them a CDA diet for 22 weeks to induce NASH and fibrosis.

First, we assessed the efficiency of the replacement of recipient Kupffer cells with donor BM cells. We transplanted BM from GFP transgenic mice and isolated the total liver nonparenchymal cell fraction. The fluorescence-activated cell sorter analysis showed that approximately 94% of F4/80-positive cells were replaced with GFP-expressing BM-derived cells (Figure 1A), indicating a very high efficiency of the replacement of Kupffer cells. Then, we examined the efficiency of the engraftment of BM cells using spleen cells from the same set of chimeric mice fed a CDA diet. Spleen cells from TLR4^{-/-} mice transplanted with wild-type BM express similar TLR4 levels to the spleen cells from whole-body wild-type mice, and the cells from wild-type mice transplanted with TLR4^{-/-} BM showed very low levels of TLR4, indicating a high efficiency of the engraftment of donor BM (Figure 1B).

The chimeric mice containing wild-type BM showed similar levels of serum alanine aminotransferase (ALT) and hepatic tumor necrosis factor (TNF) expression, whereas the chimeric mice with TLR4^{-/-} BM showed reduced ALT and hepatic TNF levels (Figure 1C-E). This result suggests that TLR4 mediates hepatocyte death likely through Kupffer cell-derived TNF. The histologic assessment of NAFLD activity score showed that wild-type recipients of TLR4^{-/-} BM and TLR4^{-/-} recipients of either wild-type or TLR4^{-/-} BM

showed reduced hepatic steatosis, suggesting that TLR4 signaling in both BM-derived cells and recipient cells contribute to hepatic steatosis (Figure 1C and F). Interestingly, TLR4^{-/-} recipients of wild-type BM and wild-type recipients of TLR4^{-/-} BM had similar levels of inflammatory cell infiltration and hepatocyte ballooning to whole-body wild-type mice (Figure 1C and F). This suggests that either wild-type BM or wild-type recipient cells are involved in TLR4-mediated liver inflammation.

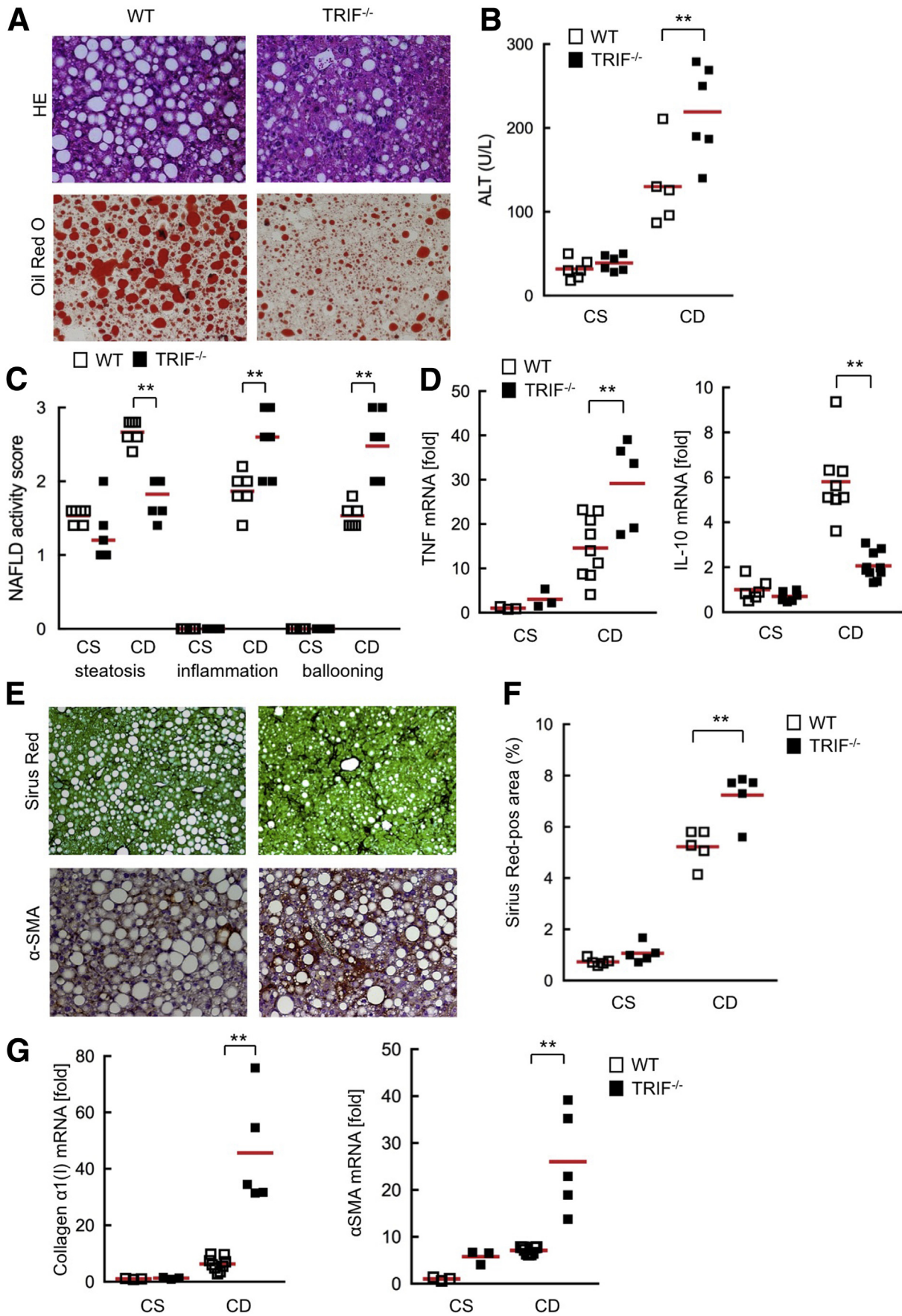
Next, we examined CDA diet-induced NASH fibrosis. The TLR4 BM chimeric mouse study showed paradoxical findings of fibrosis with hepatic steatosis and injury. The chimeric mice with wild-type resident cells (including HSCs) showed a similar degree of collagen production and α -SMA expression, whereas the chimeric mice with TLR4^{-/-} resident cells had reduced fibrosis and HSC activation (Figure 1G-I). These findings suggest that resident cells, including HSCs, are more important than BM-derived cells in the development of TLR4-mediated NASH fibrosis.

TRIF Promotes Hepatosteatosis but Inhibits Hepatic Inflammation and Fibrosis

TLR4-mediated responses are regulated by the MyD88-dependent and the TRIF-dependent pathways. Our previous study showed that MyD88 is a crucial adaptor protein for the development of NASH and fibrosis, and the function of the TRIF pathway still is unclear in NASH fibrosis.¹⁰ To investigate the role of TRIF in the development of NASH, wild-type and TRIF^{-/-} mice were subjected to 22 weeks of CDA diet feeding. TRIF^{-/-} mice showed much less hepatic steatosis than wild-type mice (Figure 2A). To our surprise, TRIF^{-/-} mice presented more inflammatory cell infiltration along with higher serum ALT levels and hepatic TNF messenger RNA expression than wild-type mice (Figure 2A-D). The expression of interleukin (IL)10, an anti-inflammatory cytokine, is regulated by the TRIF-IRF3-mediated pathway.¹² TRIF^{-/-} mice showed significantly lower IL10 expression than wild-type mice (Figure 2D). This suggests that the reduced anti-inflammatory IL10 may be an underlying mechanism of exacerbated liver inflammation and injury in TRIF^{-/-} mice.

Consistent with severe liver injury and inflammation in TRIF^{-/-} mice, these mice showed significant increases in fibrillar collagen deposition, HSC activation, and expression

Figure 1. (See previous page). **BM-derived and resident liver cells are required for TLR4-mediated hepatic steatosis, inflammation, and fibrosis in the murine NASH model induced by CDA diet.** (A) Wild-type mice were transplanted with BM from β -actin promoter-driven GFP-transgenic mice after whole-body irradiation. After 2 weeks of BMT, liposomal clodronate was injected. After 10 weeks of BMT, liver nonparenchymal cell fraction was separated and F4/80-positive GFP-expressing cells were examined by fluorescence-activated cell sorter analysis. (B-I) The TLR4 BM chimeric mice were fed the CDA diet for 22 weeks (*n* = 5-9, each). (B) The successful engraftment of donor BM cells into TLR4 BM chimeric mice was determined by TLR4 messenger RNA (mRNA) expression in spleen cells. (C) Hepatic inflammation and steatosis were evaluated by H&E staining and Oil Red O staining, respectively. Original magnification, $\times 100$ for H&E, and $\times 200$ for Oil Red O. (D) ALT levels. (E) Hepatic TNF mRNA levels were measured by quantitative PCR. (F) NAFLD activity score. (G) Liver sections were stained with Sirius Red and used for immunohistochemistry for α -SMA. Original magnification, $\times 100$ for Sirius Red staining, and $\times 200$ for α -SMA staining. (H) Quantifications of Sirius red staining. (I) Hepatic fibrogenic genes (collagen $\alpha 1$ [I], α -SMA) were determined by quantitative real-time PCR. Similar results were obtained in 2 independent experiments. A representative result is shown. **P* < .05, ***P* < .01. WT, wild type. Red horizontal bars represent average.



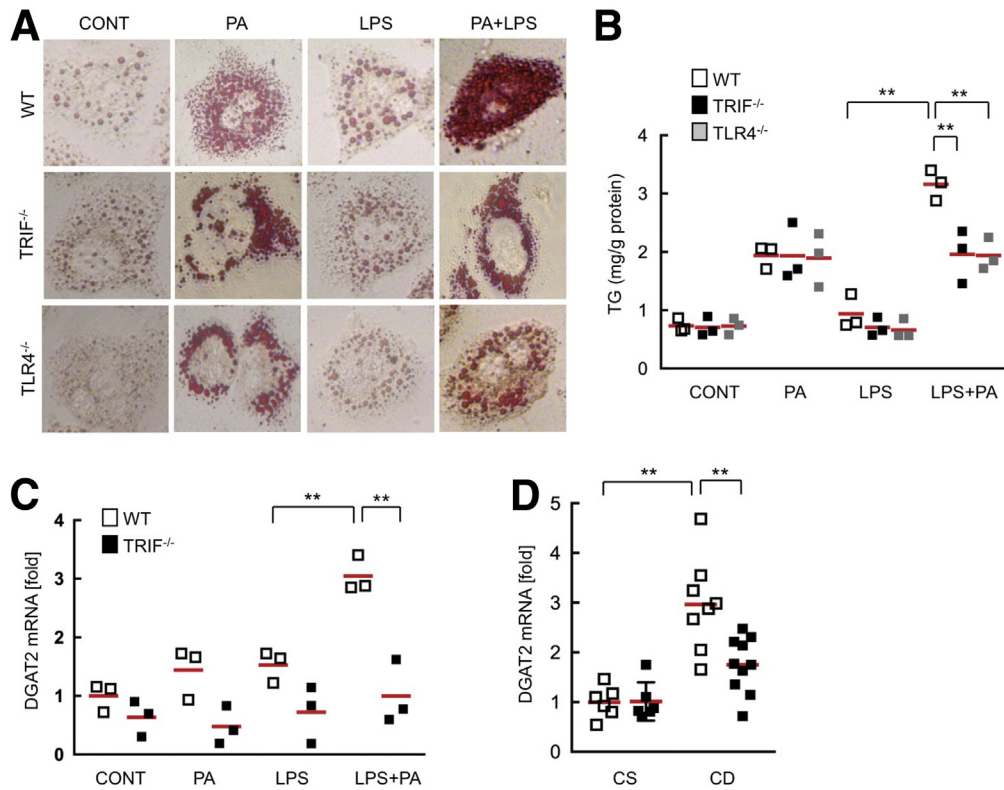


Figure 3. The TLR4–TRIF signaling enhances palmitate-induced fat accumulation in hepatocytes. Wild-type (WT), TRIF^{-/-}, and TLR4^{-/-} hepatocytes were treated with 200 μmol/L palmitate and/or 100 ng/mL LPS for 24 hours. (A) Representative pictures of Oil Red O staining. Original magnification, ×400. (B) Triglyceride (TG) concentrations in hepatocytes. (C) WT and TRIF^{-/-} hepatocytes were treated with 200 μmol/L palmitate and/or 100 ng/mL LPS for 12 hours. Messenger RNA (mRNA) expression of DGAT2 was determined by quantitative real-time PCR. Similar results were obtained in 2 independent experiments. A representative result is shown. (D) WT and TRIF^{-/-} mice were fed a choline-supplemented amino acid–defined diet (CS) or CDAA (CD) diet for 22 weeks (n = 5–9, each). Hepatic DGAT2 mRNA expression was determined by quantitative real-time PCR. *White square*, wild-type mice; *black square*, TRIF^{-/-} mice; *gray square*, TLR4^{-/-} mice. **P < .01. CONT, control; PA, palmitic acids. Red horizontal bars represent average.

of profibrogenic genes (collagen α1[I] and α-SMA) compared with wild-type mice (Figure 2E–G). These results indicate that the TRIF pathway contributes to hepatic steatosis, but negatively regulates hepatic injury, inflammation, and fibrosis. This also suggests that TRIF-mediated IL10 may play a role as a negative regulator of liver inflammation.

TLR4 Signaling Potentiates Palmitic Acid-Induced Hepatocyte Lipid Accumulation Through TRIF

TRIF^{-/-} mice showed reduced hepatic steatosis compared with wild-type mice (Figure 2A). Given that systemic endotoxin levels are increased in human NASH,^{5–7} we hypothesize

that translocated LPS is a ligand for TLR4 during NASH development. To clarify whether TLR4 and TRIF mediate lipid accumulation in hepatocytes, we treated primary hepatocytes, isolated from wild-type, TRIF^{-/-}, and TLR4^{-/-} mice, with palmitic acids and/or LPS. Palmitic acids induced lipid accumulation in all primary hepatocytes from wild-type, TRIF^{-/-}, and TLR4^{-/-} mice, whereas LPS alone did not increase lipid accumulation as assessed by Oil Red O staining (Figure 3A). When we combined the treatment with palmitic acids and LPS, only the wild-type hepatocytes showed severe lipid accumulation, whereas TRIF^{-/-} and TLR4^{-/-} hepatocytes did not (Figure 3A). Consistent with hepatocyte lipid accumulation, hepatocyte triglyceride levels were increased significantly by co-treatment with palmitate and LPS in

Figure 2. (See previous page). TRIF^{-/-} mice showed severe inflammation and fibrosis but less steatosis in the murine NASH model induced by the CDAA diet. Wild-type (WT) and TRIF^{-/-} mice were fed a choline-supplemented amino acid–defined diet (CS) or CDAA (CD) diet for 22 weeks (n = 5–9, each). (A) Liver sections were stained with H&E and Oil Red O. Original magnification, ×200 for H&E and Oil Red O staining. (B) Serum ALT levels. (C) NAFLD activity score. (D) Hepatic messenger RNA (mRNA) (TNF, IL10) expression was determined by quantitative real-time PCR. (E) Liver sections were stained with Sirius Red and used for immunohistochemistry for α-SMA. Original magnification, ×100 for Sirius Red staining, and ×200 for α-SMA staining. (F) Quantification of Sirius Red staining. (G) Hepatic fibrogenic genes (collagen α1[I], α-SMA) were determined by quantitative real-time PCR. *White square*, wild-type mice; *black square*, TRIF^{-/-} mice. Similar results were obtained in 2 independent experiments. A representative result is shown. **P < .01. Red horizontal bars represent average.

wild-type hepatocytes, and was reduced in TRIF^{-/-} as well as TLR4^{-/-} hepatocytes (Figure 3B). To examine the molecular mechanism of hepatocyte lipid accumulation potentiated by the TLR4-TRIF-mediated pathway, we measured messenger RNA expression of diacylglycerol acyltransferase 2 (DGAT2), an enzyme that converts diglyceride to triglyceride, in hepatocytes after treatment with palmitic acids and/or LPS. DGAT2 was up-regulated in wild-type, but not in TRIF^{-/-}, hepatocytes (Figure 3C). Consistently, increased DGAT2 levels in wild-type livers were reduced in TRIF^{-/-} livers (Figure 3D). These results suggest that the TLR4-TRIF pathway potentiates free fatty acid-induced lipid accumulation in hepatocytes, at least in part through DGAT2 induction.

The TLR4-TRIF Pathway Induces Death After the Sensitization of Hepatocytes With Palmitic Acids

We next investigated whether the TLR4-TRIF pathway is involved in hepatocyte death. To examine the setting of fatty

liver diseases, we examined the effect of TLR4 activation on hepatocyte death in lipid-accumulated hepatocytes. After 24 hours of palmitate treatment, wild-type, TRIF^{-/-}, and TLR4^{-/-} hepatocytes stored lipid droplets (Figure 3A). Hepatocyte apoptosis was assessed by terminal deoxynucleotidyl transferase-mediated deoxyuridine triphosphate nick-end labeling staining and measuring LDH released into the culture supernatant. In palmitate-pretreated, lipid-accumulated wild-type hepatocytes, hepatocyte apoptosis and LDH release were increased after LPS treatment, whereas these events were not seen in TRIF^{-/-} and TLR4^{-/-} lipid-accumulated hepatocytes (Figure 4A and B), indicating that the TLR4-TRIF pathway positively regulates hepatocyte death in lipid-accumulated hepatocytes. These results were inconsistent with the finding that TRIF^{-/-} mice showed increased liver injury after CDAA diet feeding. This suggests that increased liver injury in TRIF^{-/-} mice is not caused by the direct effect of the TLR4-TRIF-mediated signaling in hepatocytes and may be mediated through increased liver

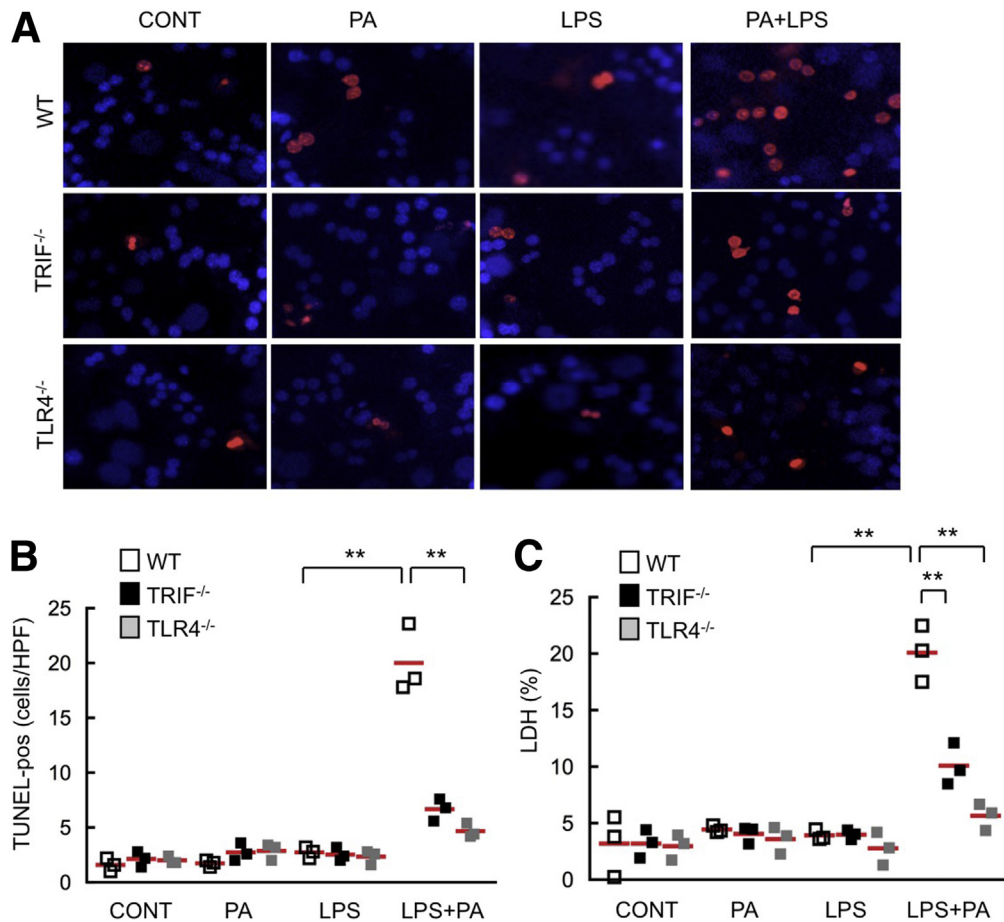


Figure 4. The TLR4-TRIF signaling promotes hepatocyte apoptosis in fat-accumulated hepatocytes. Primary hepatocytes were isolated from wild-type (WT), TRIF^{-/-}, and TLR4^{-/-} mice. Cells were treated with 200 μ mol/L palmitate for 24 hours to create fat-accumulated hepatocytes. Then, cells were treated with 100 ng/mL LPS for an additional 24 hours. (A) Representative pictures of terminal deoxynucleotidyl transferase-mediated deoxyuridine triphosphate nick-end labeling (TUNEL) staining and (B) quantifications. Original magnification, $\times 400$. (C) Concentrations of LDH released to supernatants were measured. Similar results were obtained in 2 independent experiments. A representative result is shown. White square, wild-type mice; black square, TRIF^{-/-} mice; gray square, TLR4^{-/-} mice. ** $P < .01$. CONT, control; HPF, high-power field; PA, palmitic acids. Red horizontal bars represent average.

inflammation by the augmented production of inflammatory cytokines from liver nonparenchymal cells.

C-X-C motif chemokine ligand 1 and C-C motif chemokine ligand 3 Are Produced in TRIF^{-/-} Kupffer Cells, HSCs, and Hepatocytes

TLR4 expressed on liver resident cells, including HSCs and hepatocytes, play major roles in NASH-mediated fibrosis compared with TLR4 on BM-derived cells, such as Kupffer cells (Figure 1). We hypothesize that the distinct manners in cytokine/chemokine production among Kupffer cells, HSCs, and hepatocytes may be the underlying mechanisms of increased liver inflammation in TRIF^{-/-} mice. In immune cells, including macrophages, CXCL1 and CCL3 production is dependent on MyD88, whereas CCL5 and IL10 production are mediated through the TRIF-IRF3-dependent pathway.^{12,17} We examined the role of TRIF in TLR4-mediated cytokine induction in Kupffer cells. Consistent with previous studies examining macrophages,¹⁷ TRIF^{-/-} Kupffer cells produced CXCL1 and CCL3 at similar levels to wild-type cells, whereas TRIF deficiency decreased the LPS-induced production of CCL5 and IL10 in Kupffer cells (Figure 5A). In contrast, LPS stimulation induced CCL5 production but did not increase CXCL1 and CCL3 expression in MyD88^{-/-} Kupffer cells (Figure 5B). This finding indicates that TRIF^{-/-} Kupffer cells have the capacity to produce CXCL1 and CCL3 upon TLR4 activation. Interestingly, TRIF^{-/-} HSCs produced higher levels of CXCL1 and CCL3 than wild-type HSCs (Figure 5C). CCL5 that usually is regulated through the TRIF-dependent pathway in immune cells, was up-regulated and showed higher production in TRIF^{-/-} HSCs than wild-type HSCs (Figure 5C). Surprisingly, CXCL1, CCL3, and CCL5 production were inhibited in MyD88^{-/-} HSCs (Figure 5D). We previously showed that HSC activation and Bambi down-regulation requires MyD88.¹⁴ Expectedly, TRIF deficiency did not prevent Bambi down-regulation and Timp-1 up-regulation (Figure 5C). These results suggest that TRIF does not play a major role in TLR4-mediated signaling in HSCs and that TRIF may have an inhibitory effect on the MyD88-dependent pathway in HSCs. We previously reported that hepatocytes produce neutrophil-recruiting chemokines, such as CXCL1, in response to TLR ligands.¹⁸ In wild-type hepatocytes, LPS treatment increased the production of CXCL1 and CCL3. The increases in CXCL1 and CCL3 were prevented by MyD88 deficiency, but not by TRIF deficiency (Figure 5E and F). These results show that CXCL1 and CCL3 production is not abolished by TRIF deficiency in all cell types and that TRIF^{-/-} HSCs produce higher CXCL1, CCL3, and CCL5 than the wild-type HSCs; these data further suggest that CXCL1, CCL3, and higher production of chemokines in HSCs may contribute to promoting liver inflammation in CDAA diet-fed TRIF^{-/-} mice.

Increased Infiltration of Neutrophils and Macrophages in TRIF^{-/-} Mice With NAFLD

Based on the *in vitro* findings (Figure 5), we hypothesize that increased chemokine production from HSCs and MyD88-independent chemokine production in Kupffer cells

and hepatocytes are major mechanisms of the overt inflammation and fibrosis by recruiting neutrophils and macrophages in CDAA diet-fed TRIF^{-/-} mice. Because CXCL1 is a potent neutrophil-attracting chemokine and CCL3 enables recruitment of monocytes/macrophages,^{19,20} we examined hepatic CXCL1 and CCL3 expression and infiltration of neutrophils and macrophages in wild-type and TRIF^{-/-} mice after 22 weeks of CDAA diet feeding. CXCL1 expression and neutrophil infiltration were exacerbated in TRIF^{-/-} mice compared with wild-type mice (Figure 6A and B). In addition, increased hepatic CCL3 expression and macrophage infiltration also were observed in TRIF^{-/-} mice (Figure 6C and D). These results suggest that increased hepatic CXCL1 and CCL3 expression promotes neutrophil recruitment and macrophage infiltration, respectively, which augments liver inflammation and injury in TRIF^{-/-} mice.

Insulin Resistance Is Associated With the Degree of Hepatic Steatosis and Body Weight

CDAA diet-fed TRIF^{-/-} mice showed paradoxical results in regard to hepatic steatosis and injury/inflammation/fibrosis (Figure 2). A number of human studies have suggested that the severity of liver inflammation is associated with insulin resistance in NASH patients.^{21,22} To investigate whether liver inflammation and fibrosis are involved in insulin resistance, glucose and insulin tolerance tests were examined in CDAA diet-fed wild-type and TRIF^{-/-} mice. Both glucose and insulin tolerance tests showed that insulin sensitivity was improved in TRIF^{-/-} mice compared with wild-type mice (Figure 7A and B). On the CDAA diet, the body and liver weight were slightly, but significantly, lower in TRIF^{-/-} mice compared with wild-type mice (Figure 7C and D). These results suggest that hepatic steatosis and/or body weight (adipose tissue mass) are associated with insulin resistance, whereas hepatocyte injury, inflammation, and fibrosis are less likely to be involved in insulin resistance. This indicates a dissociation between insulin resistance and liver inflammation.

Discussion

The contributions of TLR4 signaling and its activation by translocated gut-derived LPS to chronic liver diseases, including alcoholic liver disease, NAFLD, cirrhosis, and liver cancer, have been well established.^{8,23} Kupffer cells are believed to play crucial roles in TLR4-mediated alcoholic steatohepatitis and NASH development.¹¹ Although we previously described the function of TLR4 in HSC activation and liver fibrosis,¹⁴ the importance of HSCs in TLR4-mediated NASH development is poorly understood. The present study attempted to answer this question by using TLR4 wild-type and TLR4^{-/-} BM chimeric mice. TLR4 uses both MyD88-dependent and TRIF-dependent pathways to induce TLR4's biological responses. The importance of MyD88 is well accepted in NASH development, whereas TRIF-dependent IRF3 activation plays important roles in the development of alcoholic liver disease.^{10,12} The present

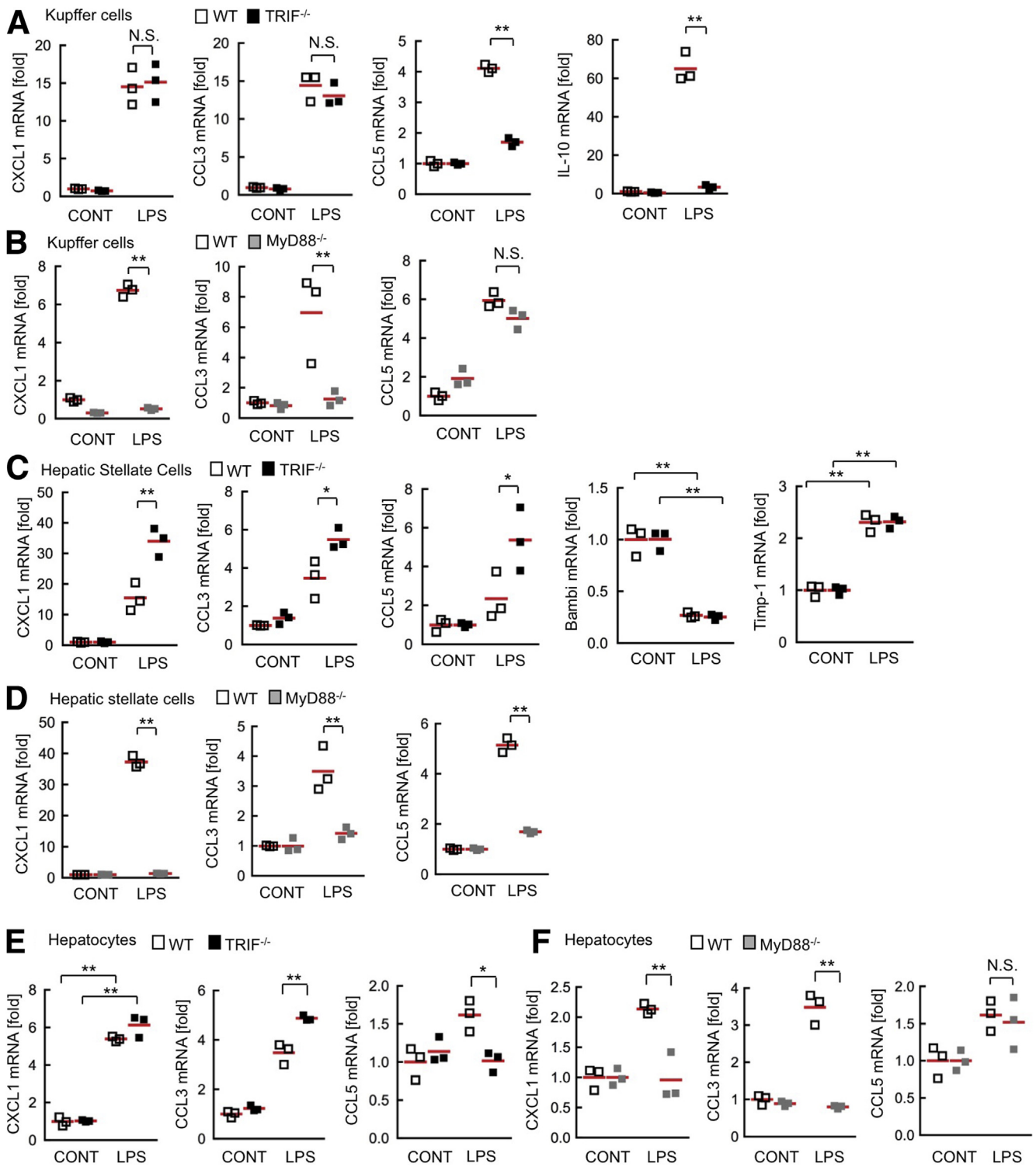


Figure 5. CXCL1 and CCL3 are produced independently of TRIF in Kupffer cells, HSCs, and hepatocytes. (A and B) Primary Kupffer cells, (C and D) HSCs, and (E and F) hepatocytes were isolated from wild-type (WT) mice, (A, C, and E) TRIF^{-/-} mice, and (B, D, and F) MyD88^{-/-} mice. Cells then were treated with LPS for 6 hours. Messenger RNA (mRNA) expression of CXCL1, CCL5, CCL3, IL10, Bambi, and Timp-1 was determined by quantitative real-time PCR. Similar results were obtained in 3 independent experiments. A representative result is shown. *White square*, wild-type mice; *black square*, TRIF^{-/-} mice; *gray square*, MyD88^{-/-} mice. **P* < .05, ***P* < .01. CONT, control; NS, not significant. Red horizontal bars represent average.

study investigated the contribution of the TLR4-TRIF pathway to NASH development.

We showed the distinct function between BM-derived cells and resident liver cells, including hepatocytes and HSCs in TLR4-mediated steatosis, hepatocyte death, inflammation, and fibrosis. Because Kupffer cells are radio-resistant cells, a standard method of generating BM chimeric mice replaces approximately 70% of Kupffer cells with BM-derived cells. However, 30% of recipient-derived Kupffer cells may be enough to contribute to liver disease progression, which often leads to the misinterpretation of the results. The yield of Kupffer cell replacement with BM cells using our technology, which performs irradiation and BM transplantation in combination with Kupffer cell depletion, is approximately 95%.²⁴ Although Kupffer cell-specific Cre transgenic mice targeting *Clec4f* were reported recently,²⁵ our method still is one of the best models to study the distinct functions of Kupffer cells and HSCs.

In conjunction with the data from TLR4 BM chimeric mice, TRIF^{-/-} mice, and a series of in vitro experiments, our

study suggests several interesting mechanisms. The TLR4 BM chimeric mouse experiment suggests that both BM-derived cells and resident cells are required for hepato-steatosis (Figure 1). TRIF^{-/-} deficiency led to reducing lipid accumulation in hepatocytes, which is at least in part mediated through DGAT2 (Figures 2 and 3). It suggests that the TLR4-TRIF pathway in hepatocytes is required for lipid accumulation and that additional Kupffer cell-derived factors enhance hepato-steatosis. In terms of hepatocyte damage, the TLR4 BM chimeric mouse study (Figure 1) suggests that TLR4 mediates hepatocyte damage through Kupffer cell-derived TNF. Although LPS-mediated hepatocyte death was decreased by TLR4 and TRIF deficiency (Figure 3), TRIF^{-/-} mice showed increased ALT levels along with increased hepatic TNF levels (Figure 3). It appears that TLR4 on immune cells, but not hepatocytes, contribute to hepatocyte death indirectly, most likely through TNF production. The assessment of the NAFLD activity score using H&E staining showed similar levels of inflammatory cell infiltration in TLR4^{-/-} recipients of wild-type BM and

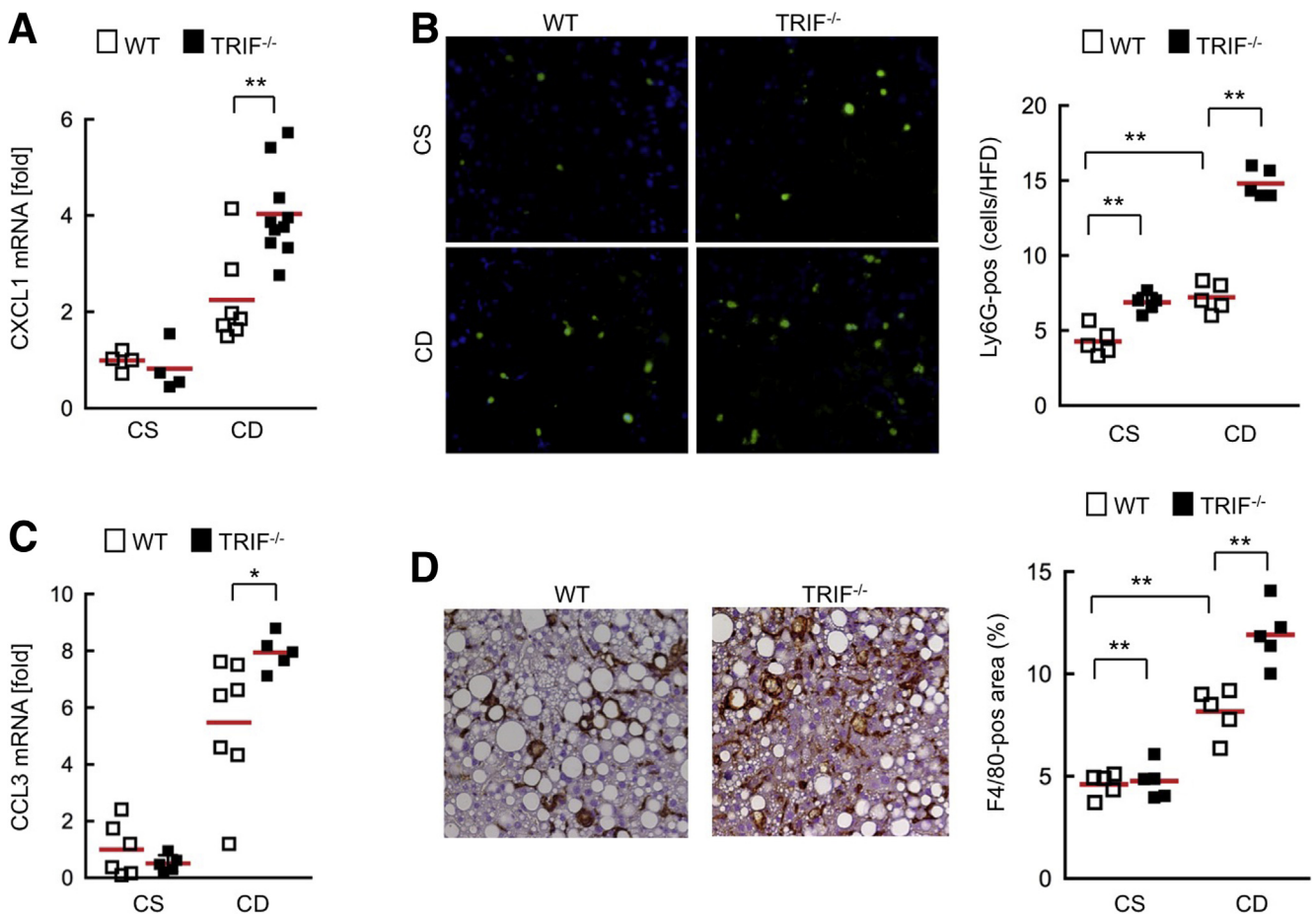


Figure 6. Increased CXCL1 and CCL3 levels accompanied by increased infiltration of neutrophils and macrophages in TRIF^{-/-} mice. Wild-type (WT) and TRIF^{-/-} mice were fed a choline-supplemented amino acid-defined diet (CS) or CDAA (CD) diet for 22 weeks (n = 4-10, each). (A) Hepatic CXCL1 messenger RNA (mRNA) expression was determined by quantitative real-time PCR. (B) Liver sections were used for immunofluorescence for Ly6G and their quantifications. Original magnification, ×200. (C) Hepatic CCL3 mRNA expression was determined by quantitative real-time PCR. (D) Liver sections were used for immunohistochemistry for F4/80 and their quantifications. Original magnification, ×200. White square, wild-type mice; black square, TRIF^{-/-} mice. *P < .05, **P < .01. Red horizontal bars represent average.

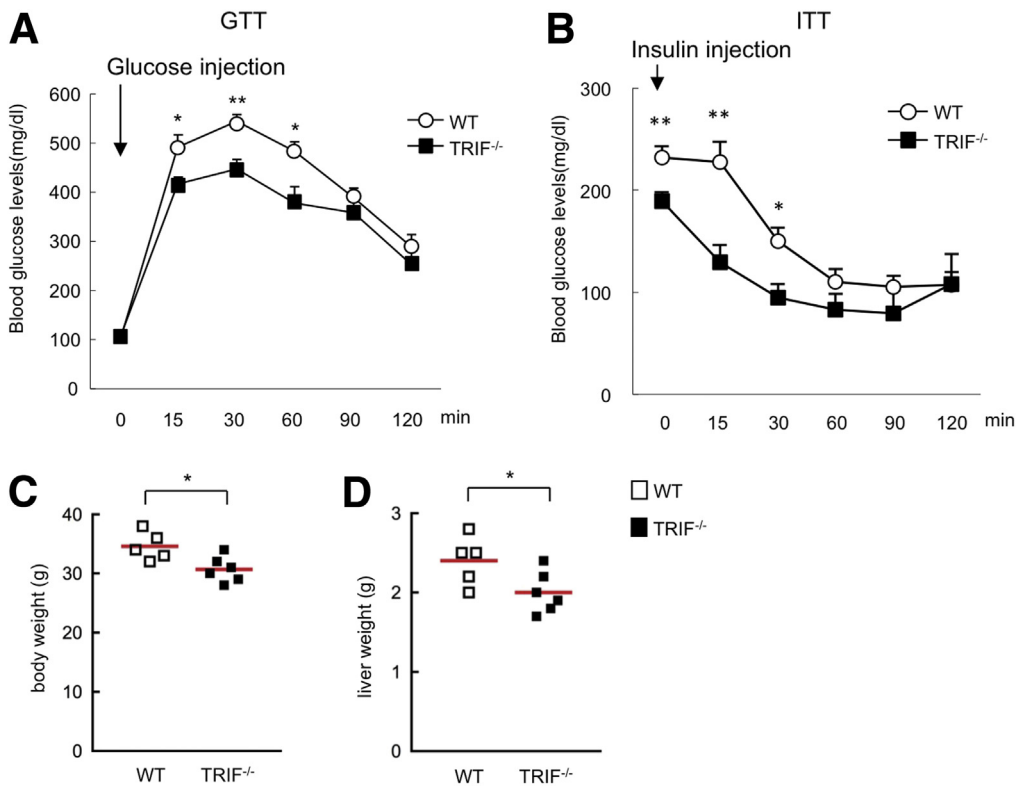


Figure 7. TRIF signaling is associated with systemic insulin resistance in mice. (A) A glucose tolerance test (GTT) and (B) an insulin tolerance test (ITT) were performed on the wild-type (WT) and TRIF^{-/-} mice fed with 22 weeks of the CDAA diet. Data represent means \pm SEM; $n = 8$ for each group. (C and D) Body weight and liver weight are shown. * $P < .05$; ** $P < .01$. Red horizontal bars represent average.

wild-type recipients of TLR4^{-/-} BM (Figure 1C and F). It is conceivable that either wild-type BM or wild-type recipient cells are involved in TLR4-mediated liver inflammation. In wild-type recipients of TLR4^{-/-} BM, cytokines/chemokines produced from wild-type recipient cells, including HSCs and hepatocytes, might affect activation of TLR4^{-/-} BM-derived immune cells, which play a role in liver inflammation. It also is possible that increased numbers of HSCs in wild-type recipients of TLR4^{-/-} BM have been determined as infiltrated inflammatory cells through H&E staining.

Compared with the high-fat diet-induced fatty liver model, the CDAA diet model recapitulated human NASH pathology well because it induces inflammatory cell infiltration, HSC activation, and fibrosis in addition to hepatosteatosis.¹⁰ Thus, the CDAA diet model is one of the suitable models for studying NASH and its related HSC activation and fibrosis. The TLR4 BM chimeric mouse study showed that TLR4 expressed on the recipient cells including HSCs is required for NASH fibrosis, suggesting that TLR4 signaling directly contributes to HSC activation, which corroborates our previous study showing HSCs as the crucial target for TLR4-mediated fibrosis.¹⁴ Interestingly, TRIF^{-/-} mice showed augmented liver fibrosis (Figure 2). This may be because the TLR4-mediated fibrogenic response, such as the up-regulation of Timp-1 and the down-regulation of Bambi, is not inhibited in TRIF^{-/-} HSCs.¹⁴ Notably, HSCs produce much higher levels of CXCL1, CCL3, and CCL5 (Figures 5 and 8). Although CCL5 is produced through the TRIF-dependent pathway in immune cells, including Kupffer cells, TRIF^{-/-} HSCs have a higher capacity

to produce CCL5 than wild-type HSCs (Figures 5 and 8). The previous study showed that TRIF in osteoblasts and osteoclasts do not play a role and showed MyD88 as the only adaptor molecule that controls TLR4-mediated pathophysiological roles in those cells.²⁶ It is conceivable that as the adaptor protein only MyD88, but not TRIF, is required for TLR4 signaling in HSCs (Figure 8). Given that TRIF^{-/-} HSCs produce higher CXCL1, CCL3, and CCL5 (Figure 5), TRIF may negatively regulate the TLR4-MyD88-dependent pathway by unidentified mechanisms.

In the present study, TRIF^{-/-} mice showed overt liver inflammation induced by the CDAA diet compared with wild-type mice. It is possible that reduced IL10 production in TRIF^{-/-} mice is one of the underlying mechanisms of exacerbated liver inflammation and injury because IL10 is a powerful anti-inflammatory cytokine that counterbalances overt inflammatory responses (Figure 8). Moreover, it has been reported that IL10^{-/-} mice had increased liver inflammation but reduced steatosis after alcohol or HFD feeding, which corroborates with the liver finding (increased liver inflammation but reduced steatosis) in TRIF^{-/-} mice.²⁷ It also is possible that higher levels of CXCL1, CCL3, and CCL5 produced by TRIF^{-/-} HSCs may be a mechanism of increased liver inflammation in TRIF^{-/-} mice. Our findings corroborate a recent study that showed hepatocytes or HSC-derived CXCL1 as crucial for recruiting neutrophils in liver diseases.^{18,19,28} Although CCL5 production is decreased in TRIF^{-/-} Kupffer cells and hepatocytes, these cells can produce similar levels of CXCL1 and CCL3 compared with wild-type cells. Thus, it is conceivable that increased production

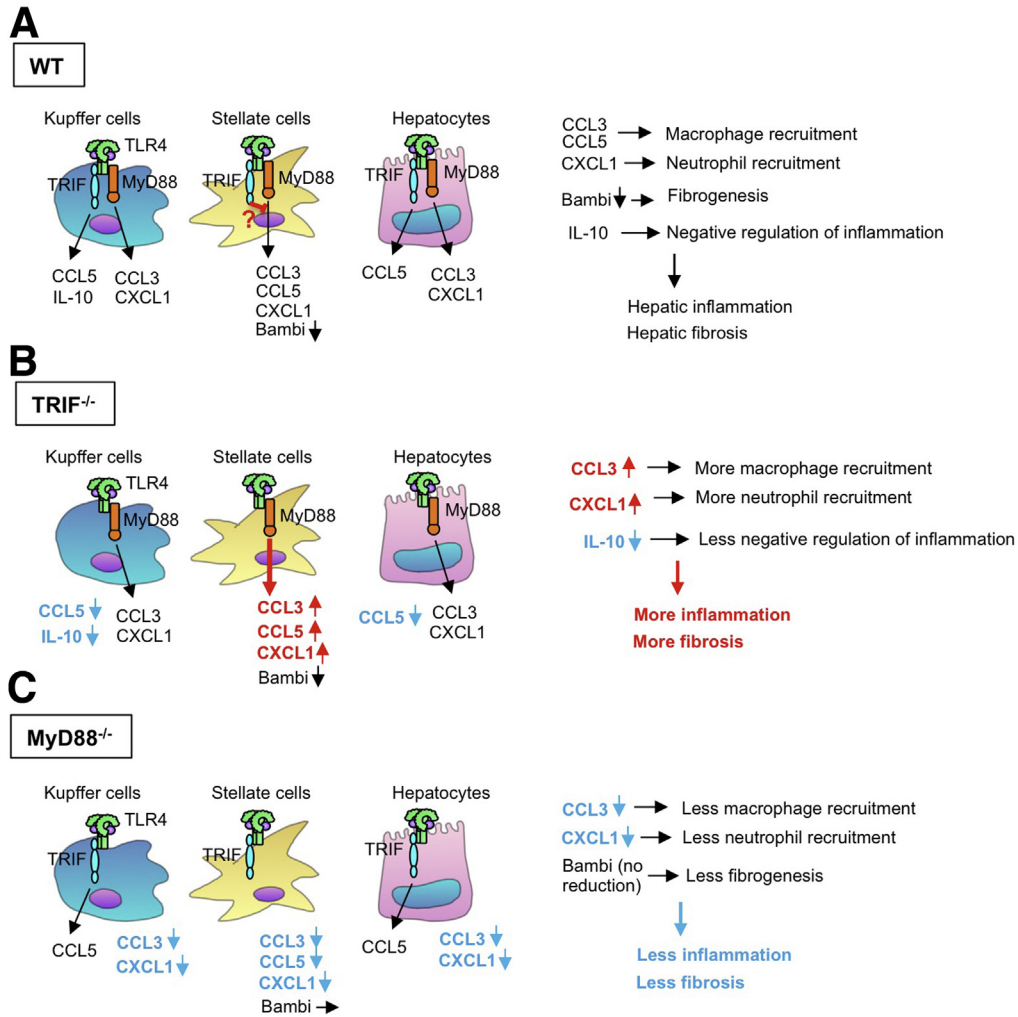


Figure 8. TRIF- and MyD88-dependent pathways control liver inflammation and fibrosis in NASH. High nutrient, choline-deficient, or obese conditions affect the composition and the amount of intestinal bacteria. In the mouse NASH model, translocated LPS stimulates TLR4 on Kupffer cells, HSCs, and hepatocytes. (A) Activated TLR4 subsequently activates MyD88-dependent and TRIF-dependent pathways. Through the MyD88-dependent pathway, Kupffer cells produce CCL3 and CXCL1, and through the TRIF-dependent pathway Kupffer cells produce CCL5 and IL10. In hepatocytes, CCL3 and CXCL1 production is MyD88-dependent whereas CCL5 induction is TRIF-dependent. In contrast, all CCL3, CCL5, and CXCL1 induction is mediated through MyD88 in HSCs. TRIF might be involved in negative regulation of MyD88-dependent chemokine induction. Bambi down-regulation is MyD88-dependent. (B) In TRIF^{-/-} conditions, Kupffer cells and hepatocytes can produce CCL3 and CXCL1, and HSCs produce higher levels of CCL3, CCL5, and CXCL1 and preserve the capacity to down-regulate Bambi. Because TRIF^{-/-} Kupffer cells do not produce IL10, hepatic inflammatory and fibrogenic responses are exacerbated. (C) In MyD88^{-/-} conditions, Kupffer cells, HSCs, and hepatocytes do not produce CXCL1 and CCL3. Bambi down-regulation does not occur in MyD88^{-/-} HSCs. Thus, hepatic inflammatory and fibrogenic responses are reduced.

of CXCL1 and CCL3 recruit neutrophils and macrophages, respectively, which exacerbates liver inflammation in TRIF^{-/-} mice (Figures 6 and 8). CCL5 produced from HSCs also can participate in immune cell recruitment.

The present study showed an interesting finding related to TRIF^{-/-} mice possessing more liver inflammation but less insulin resistance. Although there is a strong association between NASH degree and insulin resistance in human studies,^{21,22} our results suggest a dissociation between liver inflammation and insulin resistance. However, it is a noteworthy fact that there is an association of hepatic steatosis and adipose tissue mass with insulin resistance

because TRIF^{-/-} mice showed reduced hepatosteatosis and body weight compared with wild-type mice.

Another potential mechanism of the exacerbated liver inflammation and HSC activation in TRIF^{-/-} mice may be mediated through the TLR3-TRIF pathway. TLR3 uses only the TRIF-dependent pathway. TLR3-mediated natural killer cell activation is a negative regulating mechanism of liver fibrosis by killing HSCs.²⁹ It is suggested that increased HSC activation in TRIF^{-/-} mice may be mediated through the reduction of TLR3-TRIF-dependent natural killer cell killing of activated HSCs. The role of TLR3 in the development of HFD-induced obesity and insulin resistance is

controversial,^{30,31} suggesting the TLR4–TRIF pathway is a more consistent pathway for developing insulin resistance than is the TLR3–TRIF pathway.

In summary, the present study showed that TLR4 and TRIF play distinct roles in different liver cells in NASH and its related fibrosis. TLR4 and TRIF promote hepatic steatosis. TLR4 directly acts on BM-derived immune cells and HSCs to promote liver inflammation and fibrosis whereas TRIF may have an inhibitory function in liver inflammation and fibrosis through the production of IL10. In addition, TRIF-independent production of CXCL1, CCL3, and CCL5 may contribute to enhanced liver inflammation and fibrosis in TRIF^{-/-} mice (Figure 8). Moreover, we showed that hepatic steatosis and adipose tissue mass, but not hepatic inflammation and fibrosis, are associated with insulin resistance in the NASH mouse model. We suggest that a better understanding of the TLR4-TRIF-mediated pathophysiology in the liver is important for developing better management of fatty liver diseases.

References

- Day CP. Non-alcoholic fatty liver disease: a massive problem. *Clin Med (Lond)* 2011;11:176–178.
- Kneeman JM, Misdraji J, Corey KE. Secondary causes of nonalcoholic fatty liver disease. *Therap Adv Gastroenterol* 2012;5:199–207.
- Sanyal AJ, Brunt EM, Kleiner DE, et al. Endpoints and clinical trial design for nonalcoholic steatohepatitis. *Hepatology* 2011;54:344–353.
- Tiniakos DG, Vos MB, Brunt EM. Nonalcoholic fatty liver disease: pathology and pathogenesis. *Annu Rev Pathol* 2010;5:145–171.
- Schnabl B, Brenner DA. Interactions between the intestinal microbiome and liver diseases. *Gastroenterology* 2014;146:1513–1524.
- Alisi A, Manco M, Devito R, et al. Endotoxin and plasminogen activator inhibitor-1 serum levels associated with nonalcoholic steatohepatitis in children. *J Pediatr Gastroenterol Nutr* 2010;50:645–649.
- Farhadi A, Gundlapalli S, Shaikh M, et al. Susceptibility to gut leakiness: a possible mechanism for endotoxaemia in non-alcoholic steatohepatitis. *Liver Int* 2008;28:1026–1033.
- Petrasek J, Csak T, Szabo G. Toll-like receptors in liver disease. *Adv Clin Chem* 2013;59:155–201.
- Csak T, Velayudham A, Hritz I, et al. Deficiency in myeloid differentiation factor-2 and toll-like receptor 4 expression attenuates nonalcoholic steatohepatitis and fibrosis in mice. *Am J Physiol Gastrointest Liver Physiol* 2011;300:G433–G441.
- Miura K, Kodama Y, Inokuchi S, et al. Toll-like receptor 9 promotes steatohepatitis by induction of interleukin-1beta in mice. *Gastroenterology* 2010;139:323–334 e7.
- Rivera CA, Adegboyega P, van Rooijen N, et al. Toll-like receptor-4 signaling and Kupffer cells play pivotal roles in the pathogenesis of non-alcoholic steatohepatitis. *J Hepatol* 2007;47:571–579.
- Petrasek J, Dolganiuc A, Csak T, et al. Interferon regulatory factor 3 and type I interferons are protective in alcoholic liver injury in mice by way of crosstalk of parenchymal and myeloid cells. *Hepatology* 2011;53:649–660.
- Wang XA, Zhang R, She ZG, et al. Interferon regulatory factor 3 constrains IKKbeta/NF-kappaB signaling to alleviate hepatic steatosis and insulin resistance. *Hepatology* 2014;59:870–885.
- Seki E, De Minicis S, Osterreicher CH, et al. TLR4 enhances TGF-beta signaling and hepatic fibrosis. *Nat Med* 2007;13:1324–1332.
- Seki E, Tsutsui H, Nakano H, et al. Lipopolysaccharide-induced IL-18 secretion from murine Kupffer cells independently of myeloid differentiation factor 88 that is critically involved in induction of production of IL-12 and IL-1beta. *J Immunol* 2001;166:2651–2657.
- Miura K, Yang L, van Rooijen N, et al. Toll-like receptor 2 and palmitic acid cooperatively contribute to the development of nonalcoholic steatohepatitis through inflammasome activation in mice. *Hepatology* 2013;57:577–589.
- Hirotsu T, Yamamoto M, Kumagai Y, et al. Regulation of lipopolysaccharide-inducible genes by MyD88 and Toll/IL-1 domain containing adaptor inducing IFN-beta. *Biochem Biophys Res Commun* 2005;328:383–392.
- Roh YS, Zhang B, Loomba R, et al. TLR2 and TLR9 contribute to alcohol-mediated liver injury through induction of CXCL1 and neutrophil infiltration. *Am J Physiol Gastrointest Liver Physiol* 2015;309:G30–G41.
- Bigorgne AE, John B, Ebrahimkhani MR, et al. TLR4-dependent secretion by hepatic stellate cells of the neutrophil-chemoattractant CXCL1 mediates liver response to gut microbiota. *PLoS One* 2016;11:e0151063.
- Seki E, De Minicis S, Gwak GY, et al. CCR1 and CCR5 promote hepatic fibrosis in mice. *J Clin Invest* 2009;119:1858–1870.
- Loomba R, Abraham M, Unalp A, et al. Association between diabetes, family history of diabetes, and risk of nonalcoholic steatohepatitis and fibrosis. *Hepatology* 2012;56:943–951.
- Choudhury J, Sanyal AJ. Insulin resistance and the pathogenesis of nonalcoholic fatty liver disease. *Clin Liver Dis* 2004;8:575–594, ix.
- Seki E, Schwabe RF. Hepatic inflammation and fibrosis: functional links and key pathways. *Hepatology* 2015;61:1066–1079.
- Inokuchi S, Tsukamoto H, Park E, et al. Toll-like receptor 4 mediates alcohol-induced steatohepatitis through bone marrow-derived and endogenous liver cells in mice. *Alcohol Clin Exp Res* 2011;35:1509–1518.
- Scott CL, Zheng F, De Baetselier P, et al. Bone marrow-derived monocytes give rise to self-renewing and fully differentiated Kupffer cells. *Nat Commun* 2016;7:10321.
- Sato N, Takahashi N, Suda K, et al. MyD88 but not TRIF is essential for osteoclastogenesis induced by

- lipopolysaccharide, diacyl lipopeptide, and IL-1 α . *J Exp Med* 2004;200:601–611.
27. Miller AM, Wang H, Bertola A, et al. Inflammation-associated interleukin-6/signal transducer and activator of transcription 3 activation ameliorates alcoholic and nonalcoholic fatty liver diseases in interleukin-10-deficient mice. *Hepatology* 2011;54:846–856.
 28. Chang B, Xu MJ, Zhou Z, et al. Short- or long-term high-fat diet feeding plus acute ethanol binge synergistically induce acute liver injury in mice: an important role for CXCL1. *Hepatology* 2015;62:1070–1085.
 29. Jeong WI, Park O, Radaeva S, et al. STAT1 inhibits liver fibrosis in mice by inhibiting stellate cell proliferation and stimulating NK cell cytotoxicity. *Hepatology* 2006;44:1441–1451.
 30. Wu LH, Huang CC, Adhikarakunnathu S, et al. Loss of toll-like receptor 3 function improves glucose tolerance and reduces liver steatosis in obese mice. *Metabolism* 2012;61:1633–1645.
 31. Ballak DB, van Asseldonk EJ, van Diepen JA, et al. TLR-3 is present in human adipocytes, but its signalling is not required for obesity-induced inflammation in adipose tissue in vivo. *PLoS One* 2015;10:e0123152.

Received September 29, 2016. Accepted December 25, 2016.

Correspondence

Address correspondence to: Ekihiro Seki, MD, PhD, Division of Gastroenterology, Department of Medicine, Cedars-Sinai Medical Center, 8700 Beverly Boulevard, Davis Research Building, Suite 2099, Los Angeles, California 90048. e-mail: Ekihiro.Seki@cshs.org; fax: (310) 423-0157.

Acknowledgments

The authors thank Ms Daisy Gomez (Department of Medicine, Cedars-Sinai Medical Center, Los Angeles, CA) for editing the manuscript.

Ling Yang was responsible for the study concept and design, acquisition of data, analysis and interpretation of data, and drafting of the manuscript; Kouichi Miura was responsible for the study concept and design, acquisition of data, analysis and interpretation of data, and critical revision of the manuscript for important intellectual content; Bi Zhang was responsible for the study design, acquisition of data, and analysis and interpretation of data; Hiroshi Matsushita, Yoon Mee Yang, Shuang Liang, Jingyi Song, and Yoon Seok Roh were responsible for the acquisition and analysis of data; Ekihiro Seki was responsible for study supervision, the study concept and design, analysis and interpretation of data, writing of the manuscript, statistical analysis, and obtained funding.

Conflicts of interest

The authors disclose no conflicts.

Funding

This study was supported by National Institutes of Health grants R01AA02172, R01DK085252, and P42 ES010337 (E.S.); the American Liver Foundation Irwin M. Arias, MD, Postdoctoral Research Fellowship (Y.M.Y.); the American Liver Foundation Congressman John Joseph Moakley Postdoctoral Research Fellowship (Y.S.R.); and National Natural Science Foundation of China grants 81370550, 81570530, and 30500658 (L.Y.).